ECCOMAS Congress 2016
VII European Congress on Computational Methods in Applied Sciences and Engineering
M. Papadrakakis, V. Papadopoulos, G. Stefanou, V. Plevris (eds.)
Crete Island, Greece, 5–10 June 2016

ELASTOSTATIC AND MODAL AND BUCKLING ANALYSIS OF SPATIAL FGM BEAM STRUCTURES

Justín Murín[1], Mehdi Aminbaghai[2], Juraj Hrabovský[1],

Vladimír Kutiš[1], Juraj Paulech[1], Stephan Kugler[3]

[1]Slovak University of Technology in Bratislava, Faculty of Electrical Engineering and Information Technology, Ilkovicova 3, 812 19 Bratislava, Slovakia,
justin.murin@stuba.sk
[2]Institute for Mechanics of Materials and Structures Karlsplatz 13, A-1040 Vienna, Austria,
mehdi.aminbaghai@tuwien.ac.at
[3]University of Applied Sciences Wiener Neustadt, Johannes Gutenberg-Strasse 3, A/2700 Wiener Neustadt, Austria,
kugler@fhwn.ac.at

Keywords: Functionally graded materials, Homogenization of material properties, FGM finite 3D beam element, Static and modal and buckling analysis, Spatially varying material properties.

Abstract. *In this contribution, a homogenized beam finite element of double symmetric cross-section made of a Functionally Graded Material (FGM) is presented, which can be used for static, modal and buckling analysis of single beams and beam structures with three directional variation of material properties. The material properties in a real beam can vary continuously in longitudinal direction while the variation with respect the transversal and lateral directions is assumed to be symmetric in a continuous or discontinuous manner. The shear force deformation effect and the effect of inertia and rotary inertia are taken into account. Additionally, the longitudinally varying Winkler elastic foundation and the effect of axial force are included by the finite element equations as well. Homogenization of spatially varying material properties to effective quantities with a longitudinal variation is done by the extended mixture rules and multilayer method (MLM). For the homogenized beam the 12×12 finite element effective matrix, consisting of the linearized stiffness and consistent mass inertia terms, is established. Numerical experiments are made concerning static, modal and buckling analyses of single FGM beam and beam structures to show the accuracy and effectiveness of the proposed FGM beam finite element.*

1 INTRODUCTION

Important classes of structural components, where FGM is used, are beams and beam structures. FGM beams play an important role not only in classical structural applications, but we can find many applications in thermal, electric-thermal or electric-thermal-structural systems (e.g. micro-electro-mechanical systems (MEMS) as sensors and actuators and other mechatronic devices). In all these applications, using new materials like FGM can greatly improve the efficiency of the systems. FGM is built as a mixture of two or more constituents whose particles have almost the similar form and dimensions (powder, plasma particles, etc.). The continuous or multilayered variation of macroscopic material properties can be caused by varying the volume fraction of the constituents or by varying the constituent's material properties (e.g. by a non-homogeneous temperature field). In the literature a huge amount of papers can be found which deal with modeling and simulation of static and dynamic problems of FGM beams.

The latest results of theoretical research on statics and vibration and loss of stability of FGM and composite beams are presented for example in the articles [1-13].The first significant feature of the references [1-8] (and also of those published in the previous period) is that variation of material properties is considered only in one direction, usually along the beam thickness, and exceptionally in the longitudinal direction of the beam. The second feature of these works is that they are analyzed only a simple planar beams with rectangular cross-section. The third feature of most of these works is that their fundamental equations are based on the equations of plane stress state in a continuum with varying material properties which are simplified for the solution of the beams. In [9-12], general formulations for non-uniform shear warping are presented and an advanced 20×20 stiffness matrix and the corresponding nodal load vector of a member of arbitrary composite cross section is developed, taking shear lag effects into account due to both flexure and torsion. In [13], a static analysis of three-dimensional FGM beams by hierarchical modeling and a collocation meshless solution method is presented.

With regard to our work in the past period in the field, we presented in [14-16] a solution of free vibration of a single 2D FGM beam with continuous planar polynomial variation of material properties (in axial and transversal direction) by a fourth-order differential equation of second order beam theory. The focus of these publications is laid on a new concept for expanding the second order bending beam theory considering the shear deformation according to Timoshenko beam theory. There, the shear deformation effect in FGM beams with planar continuous variations of material properties is originally included by means of the average shear correction factor that has been obtained by an integration of the shear correction function [17]. A continuous polynomial variation of the effective elastic modulus and the mass density is considered by continuous polynomial planar variation of both the volume fraction and material properties of the FGM constituents. The choice of a polynomial gradation of material properties enables an easier integration of the derived differential equation and allows to model practically realizable variations of material properties. The effect of consistent inertia and rotary inertia, and the effect of axial forces are taken into account as well.

As mentioned above, many time published papers registered e.g. in the Web of Science database, deal with static and dynamic and buckling analysis of the FGM single planar beam with transverse variation of material properties only. Less attention is paid on both the longitudinal and lateral variations of material properties. The authors failed in finding more papers which deal with analysis of single beams or spatial beam structures made of FGM with spatial variation of material properties (in three directions).

The proposed contribution is a continuation of our previous papers [14-18]. The derivation of the FGM beam finite element equations suitable for static, modal and buckling analyses of single beams or spatial beam structures made of spatially varying FGM (in longitudinal and transversal and lateral direction) is presented. From the differential equations of axial, flexural and torsional deformation of the FGM beam with longitudinally varying material properties the transfer relations and following the local and global finite beam element matrices are established. Effects of axial and shear forces are included as well as the longitudinally varying Winkler elastic foundation and inertia loads. Homogenization of the spatially varying material properties in the real FGM beam and calculation of their effective values are done by extended mixture rules and by the multilayer method (MLM) [18,25]. This method can also be used in the homogenization of multilayer beams with symmetrically discontinuous (multilayered) variation of material properties in transversal and lateral direction. In the modal and buckling analysis an eigenvalue problem is solved. Numerical experiments are performed to calculate the elastostatic and modal response and the critical buckling force of chosen FGM beams and beam structures with rectangular and hollow cross-sections with spatial variations of material properties. The solution results are discussed and compared to those obtained by means of very fine 3D – solid and beam finite element meshes of the software ANSYS Workbench [34].

The novel aspects of the current paper are:

- extension of the MLM to homogenization of the spatially (polynomial) varying material properties (continuously in longitudinal and symmetrically in transversal and lateral direction (continuously or multilayered)) for calculation of the effective longitudinally varying elasticity modules for axial and flexural and torsional loading, and the competent effective mass-densities;
- extension of the second order beam theory and the uniform torsion theory on static, modal and buckling analysis of FGM beams with spatial variation of material properties (in three directions);
- including the effects of the shear and axial forces, as well as the longitudinally varying Winkler elastic foundations;
- derivation of the transfer relations for the 3D straight FGM beam (with homogenized longitudinal variation of the effective material properties) of doubly symmetric cross-section;
- establishing of the 12×12 effective finite element matrix of the 3D FGM beam (with homogenized longitudinal variation of the effective material properties) consisting of the linear and linearized geometric stiffness and consistent mass inertia terms;
- performing of the numerical experiments concerning the static and modal and buckling analysis of the FGM beams and beam structures with spatially varying material properties.

2 FINITE ELEMENT EQUATIONS OF THE 3D FGM BEAM

Let us consider a straight beam element of doubly symmetric cross-section – Figure 1. The degrees of freedom at node *i* are: the displacements u_i, v_i, w_i in the local directions *x*, *y*, *z*, and the cross-sectional area rotations about the *x*, *y*, *z* directions - $\varphi_{x,i}, \varphi_{y,i}, \varphi_{z,i}$. The degrees of freedom at the node *j* are denoted in a similar manner. The internal forces at node *i* are: the axial force N_i, the transversal forces $R_{y,i}$ and $R_{z,i}$, the bending moments $M_{y,i}$ and, the torsion moment $M_{x,i}$.

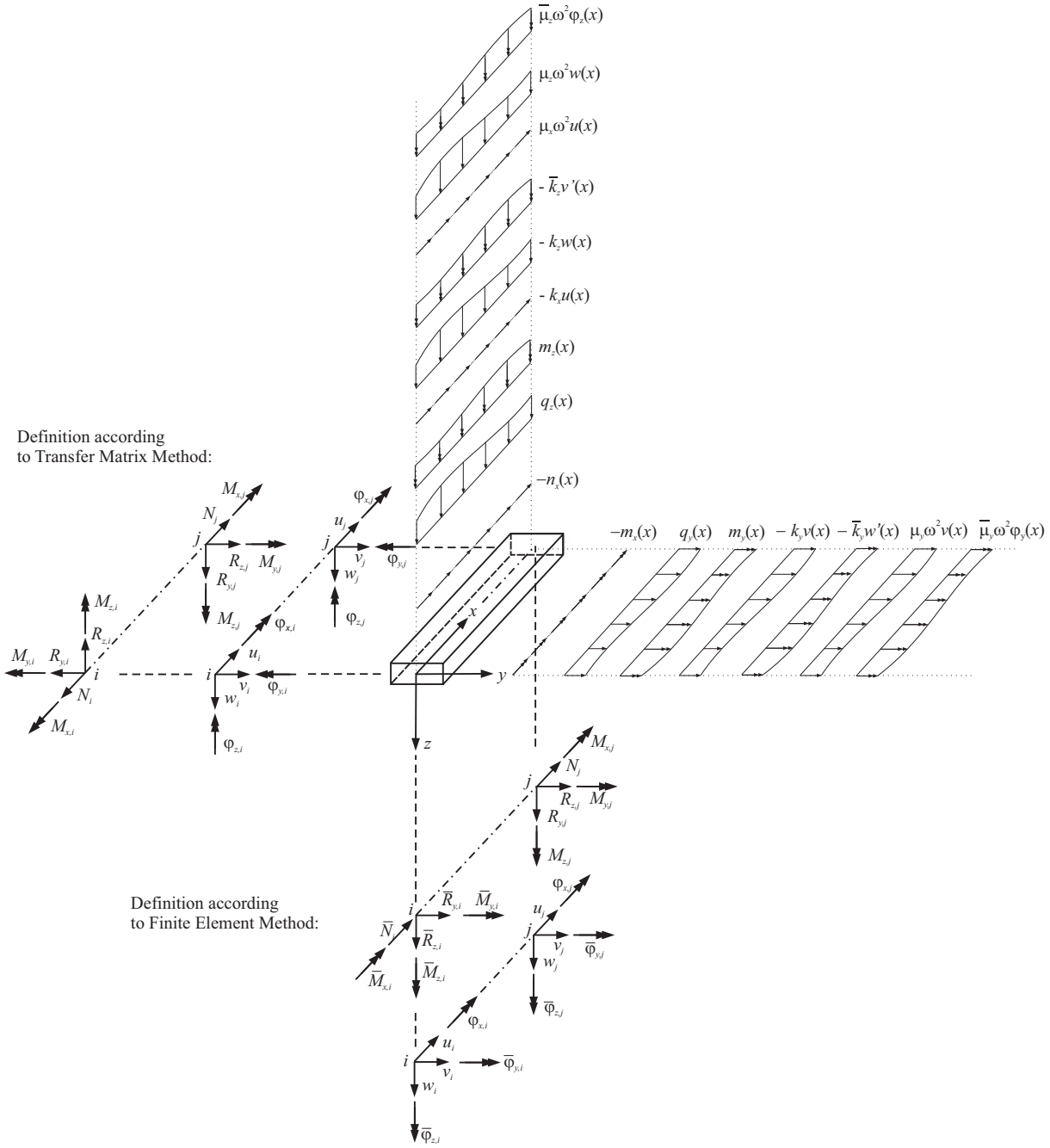

Figure 1: The local internal variables, static and inertia and loads for transfer matrix and finite element methods.

Furthermore, $n_x = n_x(x)$ denotes the axial force distribution, $q_z = q_z(x)$ and $q_y = q_y(x)$ are the transversal and lateral force distributions, $m_x = m_x(x)$, $m_y = m_y(x)$ and $m_z = m_z(x)$ are the distributed moments, $\mu_x = \rho A = \mu_y = \mu_z = \mu$ denote the mass distribution, $\overline{\mu}_y = \rho I_y$, $\overline{\mu}_z = \rho I_z$ and $\overline{\mu}_{xT} = \rho I_p$ refer to the distributions of mass moments of inertia, $\rho = \rho_L^H(x) \equiv \rho_L^H$ is the homogenized effective mass density distribution, A is the cross-sectional area, I_y and I_z are the second moments of area, $I_p = I_y + I_z$ denotes the polar moment of area, $k_x = k_x(x)$, $k_y = k_y(x)$, $k_z = k_z(x)$, $\overline{k}_y = \overline{k}_y(x)$, $\overline{k}_z = \overline{k}_z(x)$ are the elastic foundation modules

(the torsional elastic foundation is not considered), and ω is the circular frequency. The effective homogenized and longitudinally varying stiffness reads as follows: $EA = E_L^{NH}(x)A$ is the axial stiffness ($E_L^{NH}(x) \equiv E_L^{NH}$ is the effective elastic modulus for axial loading), $EI_y = E_L^{M_yH}(x)I_y$ is the flexural stiffness about the *y*-axis ($E_L^{M_yH}(x) \equiv E_L^{M_yH}$ is the effective elastic modulus for bending about axis *y*), $EI_z = E_L^{M_zH}(x)I_z$ is the flexural stiffness in axis *z*, ($E_L^{M_zH}(x) \equiv E_L^{M_zH}$ is the effective elastic modulus for bending about axis *z*), $G\bar{A}_y = G_{Ly}^{H}(x)k_y^{sm}A$ is the reduced shear stiffness in *y*-direction ($G_{Ly}^{H}(x) \equiv G_{Ly}^{H}$ is the effective shear modulus and k_y^{sm} is the average shear correction factor in *y*-direction), $G\bar{A}_z = G_{Lz}^{H}(x)k_z^{sm}A$ is the reduced shear stiffness in *z* – direction ($G_{Lz}^{H}(x) \equiv G_{Lz}^{H}$ is the effective shear modulus and k_z^{sm} is the average shear correction factor in *z* - direction), $G_L^{M_xH}(x)I_T$ is the effective torsional stiffness, $G_L^{M_xH}(x) = G_L^{M_xH}$ is the torsional elastic modulus and I_T is the torsion constant – $I_p = I_T$ for the circular and ring cross-section). The derivatives with respect to *x* of the relevant variable is denoted with an apostrophe " ′ " throughout the article.

The differential equations for axial, transversal, lateral and torsional deformation and their solution are established according the Figure 1: Definition according the Transfer Matrix Method. The finite element equations of the 3D FGM beam are established from the transfer matrix relations according Figure 1: Definition according the Finite Element Method.

2.1 Axial deformation

Equation (1) results from the axial deformation problem of the FGM beam, including the specific case of harmonic oscillations ($u = u(x)$ is the axial displacement distribution, $u' = u'(x)$ is its first derivative and $u'' = u''(x)$ is its second derivative):

$$N' = n_x + \left(k_x - \mu_x \omega^2\right)u\,, \tag{1}$$

$$u' = \frac{N}{EA}, \tag{2}$$

By combination of (1) and (2) we get the differential equation with non-constant polynomial coefficients

$$\eta_{2u}u'' + \eta_{1u}u' + \eta_{0u}u = n_x\,, \tag{3}$$

with $\eta_{2u} = EA,\ \eta_{1u} = E'A,\ \eta_{0u} = \mu\omega^2 - k_x$, and $E \equiv E_L^{NH}(x)$. The polynomial distributed axial force is: $n_x = \sum_{k=0}^{p_n} n_{x,k}x^k = n_{x,0}x^0 + n_{x,1}x^1 + n_{x,2}x^2 + \ldots + n_{x,p_n}x^{p_n}$, where $n_{x,k}$ are the values of the *k*-th derivative of the axial force n_x at the beam node *i*. For the modal analysis of axial vibration the right hand side of (3) vanishes.

The solution of (3) can be expressed by the polynomial transfer functions $\bar{b}_{kN} = \bar{b}_{kN}(x)$, ($k \in \langle 0, p_n + 2\rangle$) for axial loading [19, 20]:

$$\begin{bmatrix} u(x) \\ u'(x) \end{bmatrix} = \begin{bmatrix} \bar{b}_{0N} & \bar{b}_{1N} \\ \bar{b}'_{0N} & \bar{b}'_{1N} \end{bmatrix} \cdot \begin{bmatrix} u_i \\ u'_i \end{bmatrix} + \begin{bmatrix} \sum_{k=0}^{p_n} n_{x,k} \bar{b}_{k+2N} \\ \sum_{k=0}^{p_n} n_{x,k} \bar{b}'_{k+2N} \end{bmatrix}. \tag{4}$$

Here, u_i is the axial displacement and u'_i is the value of first derivative of $u(x)$ at node *i*.

If the $u'(x)$ and u'_i are replaced with the constitutive equation of the FGM beam (2), we get

$$\begin{bmatrix} u(x) \\ N(x) \end{bmatrix} = \begin{bmatrix} A_{1,1} = \bar{b}_{0N} & A_{1,2} = \dfrac{\bar{b}_{1N}}{E_i A} \\ A_{2,1} = EA\bar{b}'_{0N} & A_{2,2} = \dfrac{EA}{E_i A}\bar{b}'_{1N} \end{bmatrix} \cdot \begin{bmatrix} u_i \\ N_i \end{bmatrix} + \begin{bmatrix} A_{1,3} = \sum_{k=0}^{p_n} n_{x,k} \bar{b}_{k+2N} \\ A_{2,3} = EA \sum_{k=0}^{p_n} n_{x,k} \bar{b}'_{k+2N} \end{bmatrix}, \tag{5}$$

where E_i is the initial value of the homogenized elastic modulus $E_L^{NH}(x)$ at node *i*.

By setting $x = L$ in (5), the dependence of the nodal variables at node *j* on the nodal variables at node *i* are obtained. By appropriated mathematical operations and by considering the altered orientation of the local internal variables in FEM formulation (see Fig. 1), the local finite element equation for the axial loading (including the particular case of axial harmonic vibrations) are obtained (with $\bar{N}_i = -N_i$):

$$\begin{bmatrix} \bar{N}_i \\ N_j \end{bmatrix} = \begin{bmatrix} B_{1,1} = \dfrac{A_{1,1}}{A_{1,2}} & B_{1,7} = -\dfrac{1}{A_{1,2}} \\ B_{7,1} = A_{2,1} - \dfrac{A_{1,1}A_{2,2}}{A_{12}} & B_{7,7} = \dfrac{A_{2,2}}{A_{1,2}} \end{bmatrix} \cdot \begin{bmatrix} u_i \\ u_j \end{bmatrix} + \begin{bmatrix} F_1 = \dfrac{A_{1,3}}{A_{1,2}} \\ F_7 = A_{2,3} - \dfrac{A_{1,3}A_{2,2}}{A_{1,2}} \end{bmatrix}. \tag{6}$$

It can be easy shown that the matrix *B* is symmetric. The terms of the matrix *B*and the loads vector *F* are calculated numerically using MATHEMATICA [21]. Their indices are deliberately numbered in order to indicate the position of the components in the local matrix and loads vector of the 3D beam finite element, which is established later.

2.2 Flexural deformation about the *y* and *z* axis

The differential equation of 4th order with non-constant coefficients of the homogenized FGM beam flexural transversal deformation (including the particular case of flexural harmonic vibrations) in the *x*-*z* plane (Figure 1) has the form [15]:

$$\eta_{4w} w'''' + \eta_{3w} w''' + \eta_{2w} w'' + \eta_{1w} w' + \eta_{0w} w = \eta_{Lxz}(x) \tag{7}$$

with polynomial loads acting in the *x*-*z* plane

$$\eta_{Lxz}(x) = \sum_{s=0}^{\max s} \eta_{Lxz,s} x^s = \sum_{k=0}^{p_{qz}} q_{z,k} x^k + \sum_{k=1}^{p_{qz}} k q_{z,k} x^{k-1} + \sum_{k=2}^{p_{qz}} k(k-1) q_{z,k} x^{k-2} + \sum_{k=0}^{p_{my}} m_{y,k} x^k + \sum_{k=1}^{p_{my}} k m_{y,k} x^{k-1}, \tag{8}$$

where: $\eta_{Lxz,s}$ are the values of the *k*-th derivative of load polynomial (8) at the beam node *i* (*s* is the maximum degree of the polynomial); $q_{z,k}$ are the values of the *k*-th derivative of the

polynomial transversal force $q_z = q_z(x)$, and $m_{y,k}$ are the values of the *k*-th derivative of the polynomial moment $m_y = m_y(x)$ at the beam node *i* (p_{qz} and p_{my} is the maximum degree of the polynomials).For the modal analysis of flexural vibration the right hand side of (7) vanishes. Again, $w = w(x)$ refers to the deflection curve in the $x-z$ plane. The derivation of the non-constant coefficients η_{0w} to η_{4w} and appropriated parameters of the differential equation (7) from the main coupled equations (9) and (10) of the 2nd order beam theory (including the inertia forces, shear and axial force) using the relation between the transversal and shear force (11) is described in [15, 17].

$$R_z' = -q_z + k_z w - \mu\omega^2 w \qquad M_y' = Q_z + m_y + \overline{\mu_y}\omega^2\varphi_y \tag{9}$$

$$\varphi_y' = -\frac{M_y}{EI_y} \Rightarrow M_y = -EI_y\varphi_y'^{e} \quad w' = \varphi_y + \frac{Q_z}{G\overline{A}_z} \Rightarrow Q_z = G\overline{A}_z w' - G\overline{A}_z\varphi_y \tag{10}$$

$$Q_z = -\left(\overline{k_z} + N^{II}\right)w' + R_z \tag{11}$$

Here, Q_z is the shear force and $N^{II} \equiv N$ is the resultant axial force of the 2nd order beam theory (it has a system character and has to be known). In our case, $E \equiv E_L^{M_y H}$ is the homogenized elastic modulus for bending about *y* and $G \equiv G_{Lz}^{H}$ is the shear modulus in *z*-direction. Further, $\varphi_y = \varphi_y(x)$ denotes the angle of cross-section rotation about the*y*-axis.

If the variation of the beam parameters is polynomial, the solution of the differential equation (7) based on the transfer functions [20] can be written as,

$$\begin{bmatrix} w(x) \\ w'(x) \\ w''(x) \\ w'''(x) \end{bmatrix} = \begin{bmatrix} b_{0w} & b_{1w} & b_{2w} & b_{3w} \\ b_{0w}' & b_{1w}' & b_{2w}' & b_{3w}' \\ b_{0w}'' & b_{w1}'' & b_{2w}'' & b_{3w}'' \\ b_{0w}''' & b_{1w}''' & b_{2w}''' & b_{3w}''' \end{bmatrix} \cdot \begin{bmatrix} w_i \\ w_i' \\ w_i'' \\ w_i''' \end{bmatrix} + \begin{bmatrix} \sum_{s=0}^{max\,s} \eta_{Lxz,s} b_{s+4w} \\ \sum_{s=0}^{max\,s} \eta_{Lxz,s} b_{s+4w}' \\ \sum_{s=0}^{max\,s} \eta_{Lxz,s} b_{s+4w}'' \\ \sum_{s=0}^{max\,s} \eta_{Lxz,s} b_{s+4w}''' \end{bmatrix}. \tag{12}$$

There, b_{jw}, b_{jw}', b_{jw}'' and b_{jw}''' with ($j \in \langle 0,3 \rangle$),and b_{s+4w}, b_{s+4w}', b_{s+4w}'' and b_{s+4w}''' are the solution functions (so called the transfer functions for bending) of the differential equation (7). The dependence of the $w' = w'(x)$, $w'' = w''(x)$ and $w''' = w'''(x)$ on the $\varphi_y = \varphi_y(x)$, $M_y = M_y(x)$ and $R_z = R_z(x)$ is described in [648], from which the transfer matrix expression is obtained

$$\begin{bmatrix} w(x) \\ \varphi_y(x) \\ M_y(x) \\ R_z(x) \end{bmatrix} = \begin{bmatrix} A_{1,1} & A_{1,2} & A_{1,3} & A_{1,4} \\ A_{2,1} & A_{2,2} & A_{2,3} & A_{2,4} \\ A_{3,1} & A_{3,2} & A_{3,3} & A_{3,4} \\ A_{4,1} & A_{4,2} & A_{4,3} & A_{4,4} \end{bmatrix} \cdot \begin{bmatrix} w_i \\ \varphi_{y,i} \\ M_{y,i} \\ R_{z,i} \end{bmatrix} + \begin{bmatrix} A_{1,5} \\ A_{2,5} \\ A_{3,5} \\ A_{4,5} \end{bmatrix}. \tag{13}$$

The kinematical and kinetic variables at node *I* are denoted by index *i* in (12). The terms *A* in (12) are established semi analytically using MATHEMATICA [21].

By setting $x = L$ in (13) the dependence of the nodal variables at node *j* on the nodal variables at node *i* are obtained. Then, using appropriate mathematical operations and by considering the altered orientation of the local internal variables in FEM formulation (see Fig. 1), the local finite element equations for the deflection (in particular case for the flexural free vibration) about the *y*-axis read (with $\bar{R}_{z,i} = -R_{z,i}$, $\bar{M}_{y,i} = -M_{y,i}$, $\bar{\varphi}_{y,i} = -\varphi_{y,i}$ and $\bar{\varphi}_{y,j} = -\varphi_{y,j}$),

$$\begin{bmatrix} \bar{R}_{z,i} \\ \bar{M}_{y,i} \\ R_{z,j} \\ M_{y,j} \end{bmatrix} = \begin{bmatrix} B_{3,3} & B_{3,6} & B_{3,9} & B_{3,12} \\ B_{5,2} & B_{5,5} & B_{5,8} & B_{5,11} \\ B_{9,3} & B_{9,6} & B_{9,9} & B_{9,12} \\ B_{11,2} & B_{11,5} & B_{11,8} & B_{11,11} \end{bmatrix} . \begin{bmatrix} w_i \\ \bar{\varphi}_{y,i} \\ w_j \\ \bar{\varphi}_{y,j} \end{bmatrix} + \begin{bmatrix} F_3 \\ F_5 \\ F_9 \\ F_{11} \end{bmatrix} . \tag{14}$$

Indices in matrix B and *F*are deliberately numbered to indicate the position of members of the components in the local matrix of 3D beam finite element, which is shown later. The terms of matrix B and F have to be evaluated numerically. It can be easy shown that the matrix *B* is symmetric.

The differential equation of 4th order with non-constant coefficients for the homogenized FGM beam flexural deformation (including the particular case of lateral flexural harmonic vibrations) in the *x*-*y* plane (Figure 1), can be derived similarly to the previous case:

$$\eta_{4v} v'''' + \eta_{3v} v''' + \eta_{2v} v'' + \eta_{1v} v' + \eta_{0v} v = \eta_{Lxy}(x), \tag{15}$$

with polynomial loads acting in the *x*-*y* plane

$$\eta_{Lxy}(x) = \sum_{s=0}^{\max s} \eta_{Lxy,s} x^s = \sum_{k=0}^{p_{qz}} q_{y,k} x^k + \sum_{k=1}^{p_{qz}} k q_{y,k} x^{k-1} + \sum_{k=2}^{p_{qz}} k(k-1) q_{y,k} x^{k-2} + \sum_{k=0}^{p_m} m_{z,k} x^k + \sum_{k=1}^{p_m} k m_{z,k} x^{k-1}, \tag{16}$$

where: $\eta_{Lxy,s}$ are the values of the *k*-th derivative of load polynomial (16) at the beam node *i* (*s* is the maximum degree of the polynomial); $q_{y,k}$ are the values of the *k*-th derivative of the polynomial transversal force $q_y = q_y(x)$ and $m_{z,k}$ are the values of the *k*-th derivative of the polynomial moment $m_z = m_z(x)$ at the beam node *i* (p_{qy} and p_{mz} is the maximum degree of the polynomials).). For the modal analysis of flexural vibration the right hand side of (15) vanishes.

Again, $v = v(x)$ is the deflection curve in $x - y$ plane. Its derivatives with respect to *x* are denoted by an apostrophe.

By appropriated mathematical operations (similarly to the previous case) the local finite element equations for the flexural lateral deflection (in *x*-*y* plane) are obtained,

$$\begin{bmatrix} \bar{R}_{y,i} \\ \bar{M}_{z,i} \\ R_{y,j} \\ M_{z,j} \end{bmatrix} = \begin{bmatrix} B_{2,2} & B_{2,6} & B_{2,8} & B_{2,12} \\ B_{6,2} & B_{6,6} & B_{6,8} & B_{6,12} \\ B_{8,2} & B_{8,6} & B_{8,8} & B_{8,12} \\ B_{12,2} & B_{12,6} & B_{12,8} & B_{12,12} \end{bmatrix} . \begin{bmatrix} v_i \\ \bar{\varphi}_{z,i} \\ v_j \\ \bar{\varphi}_{z,j} \end{bmatrix} + \begin{bmatrix} F_2 \\ F_6 \\ F_8 \\ F_{12} \end{bmatrix} . \tag{17}$$

It can be easy shown that the matrix *B* is symmetric.

2.3 Uniform torsional deformation

The differential equations of uniform torsion of a beam are formulated according the Figure 1 and have a form,

$$M_x' = m_x - \rho_L^H I_p \omega^2 \varphi_x, \tag{18}$$

$$\varphi_x' = \frac{M_x}{GI_T}. \tag{19}$$

Here, $\varphi_x = \varphi_x(x)$ is the angle of twist about x - axis and $\varphi_x' = \varphi_x'(x)$ is its first derivative.

By a combination of equations (18) and (19) and after some mathematical manipulations the differential equation for uniform torsion (including the particular case of torsional harmonic vibrations) has been obtained

$$\eta_{2T}\varphi_x'' + \eta_{1T}\varphi_x' + \eta_{0T}\varphi_x = m_x, \tag{20}$$

with non-constant parameters $\eta_{1T} = GI_T$, $\eta_{2T} = G'I_T$, $\eta_{0T} = \rho_L^H I_p \omega^2$ and $G \equiv G_L^{M_x H}$. Further, $\varphi_x'' = \varphi_x''(x)$ is the second derivative of the angle of twist. The polynomial distributed axial force is: $m_x = \sum_{k=0}^{p_n} m_{x,k} x^k = m_{x,0}x^0 + m_{x,1}x^1 + m_{x,2}x^2 + ... + m_{x,p_n}x^{p_{mx}}$, where $m_{x,k}$ are the values of the k-th derivative of the distributed torsional moment m_x at the beam node i. For the modal analysis of axial vibration the right hand side of (3) vanishes. According to [19], the solution of the differential equation (20) reads:

$$\begin{bmatrix} \varphi_x(x) \\ \varphi_x'(x) \end{bmatrix} = \begin{bmatrix} \bar{b}_{0T} & \bar{b}_{1T} \\ \bar{b}_{0T}' & \bar{b}_{1T}' \end{bmatrix} \cdot \begin{bmatrix} \phi_{x,i} \\ \phi_{x,i}' \end{bmatrix} + \begin{bmatrix} \sum_{k=0}^{p_{mx}} m_{x,k} \bar{b}_{k+2T} \\ \sum_{k=0}^{p_{mx}} m_{x,k} \bar{b}_{k+2T}' \end{bmatrix}. \tag{21}$$

In equation (21), the $\bar{b}_{kT}$ and $\bar{b}_{kT}'$, $(k \in \langle 0, p_{mx}+2 \rangle)$, are the transfer functions for torsion and their first derivatives, respectively and represent the solution functions of the differential equation (20). The transfer functions depend on the longitudinal variation of the torsional shear modulus, the natural frequency, the polar moment of inertia, the torsion constant and the consistent mass density. They are calculated in a similar way as is shown in the previous loading cases. By inserting (18) and (19) into (21) and after some mathematical manipulations the transfer matrix relations (22) for the particular case of uniform torsion harmonic free vibration are obtained,

$$\begin{bmatrix} \varphi_x(x) \\ M_x(x) \end{bmatrix} = \begin{bmatrix} \bar{b}_{0T} & \dfrac{\bar{b}_{1T}}{G_i I_T} \\ GI_T \bar{b}_{0T}' & \dfrac{GI_T}{G_i I_T} \bar{b}_{1T}' \end{bmatrix} \cdot \begin{bmatrix} \phi_{x,i} \\ M_{x,i} \end{bmatrix} + \begin{bmatrix} A_{1,3} = \sum_{k=0}^{p_{mx}} m_{x,k} \bar{b}_{k+2T} \\ A_{2,3} = GI \sum_{k=0}^{p_{mx}} m_{x,k} \bar{b}_{k+2T}' \end{bmatrix}. \tag{22}$$

By setting $x = L$ in (22) a dependence of the state variables at point j on the state variables at initial point i for modal analysis reads

$$\begin{bmatrix} \varphi_{x,j} \\ M_{x,j} \end{bmatrix} = \begin{bmatrix} \left[\bar{b}_{0T}\right]_{x=L} & \dfrac{\left[\bar{b}_{1T}\right]_{x=L}}{G_i I_T} \\ G_j I_T \left[\bar{b}'_{0T}\right]_{x=L} & \dfrac{G_j I_T}{G_i I_T}\left[\bar{b}'_{1T}\right]_{x=L} \end{bmatrix} \cdot \begin{bmatrix} \varphi_{x,i} \\ M_{x,i} \end{bmatrix} + \begin{bmatrix} \sum_{k=0}^{p_{mx}} m_{x,k}\, \bar{b}_{k+2T}\big|_{x=L} \\ GI \sum_{k=0}^{p_{mx}} m_{x,k}\, \bar{b}'_{k+2T}\big|_{x=L} \end{bmatrix}. \tag{23}$$

By simple mathematical manipulations we get the local finite element equation for uniform torsion (with $\bar{M}_{x,i} = -M_{x,i}$):

$$\begin{bmatrix} \bar{M}_{x,i} \\ M_{x,j} \end{bmatrix} = \begin{bmatrix} B_{4,4} & B_{4,10} \\ B_{10,4} & B_{10,10} \end{bmatrix} \cdot \begin{bmatrix} \varphi_{x,i} \\ \varphi_{x,j} \end{bmatrix} + \begin{bmatrix} F_4 = \dfrac{A_{1,3}}{A_{1,2}} \\ F_{10} = A_{2,3} - \dfrac{A_{1,3}A_{2,2}}{A_{1,2}} \end{bmatrix}. \tag{24}$$

The transfer constants $\left[\bar{b}_{kT}\right]_{x=L}$ and $\left[\bar{b}'_{kT}\right]_{x=L}$, $\left(k \in \langle 0, p_{mx}+2\rangle\right)$, can be calculated with a simple numerical algorithm [20] which we programmed using software[21]. The variables G_i and G_j correspond to the values of the homogenized torsional shear modulus at point *i*and*j*. It can be easy shown that the matrix *B* is symmetric. The case of non-uniform torsion will be considered in our future work.

2.4 Local FGM beam finite element equation

The local equation of the FGM finite beam element is obtained by superposition of the equations for axial, flexural, lateral and torsional deformation, and it reads,

$$\begin{bmatrix} \bar{N}_i \\ \bar{R}_{y,i} \\ \bar{R}_{z,i} \\ \bar{M}_{x,i} \\ \bar{M}_{y,i} \\ \bar{M}_{z,i} \\ N_j \\ R_{y,j} \\ R_{z,j} \\ M_{x,j} \\ M_{y,j} \\ M_{z,j} \end{bmatrix} = \begin{bmatrix} B_{1,1} & 0 & 0 & 0 & 0 & 0 & B_{1,7} & 0 & 0 & 0 & 0 & 0 \\ & B_{2,2} & 0 & 0 & 0 & B_{2,6} & 0 & B_{2,8} & 0 & 0 & 0 & B_{2,12} \\ & & B_{3,3} & 0 & B_{3,5} & 0 & 0 & 0 & B_{3,9} & 0 & B_{3,11} & 0 \\ & & & B_{4,4} & 0 & 0 & 0 & 0 & 0 & B_{4,10} & 0 & 0 \\ & S & & & B_{5,5} & 0 & 0 & 0 & B_{5,9} & 0 & B_{5,11} & 0 \\ & & Y & & & B_{6,6} & 0 & B_{6,8} & 0 & 0 & 0 & B_{6,12} \\ & & & M & & & B_{7,7} & 0 & 0 & 0 & 0 & 0 \\ & & & & M & & & B_{8,8} & 0 & 0 & 0 & B_{8,12} \\ & & & & & E & & & B_{9,9} & 0 & B_{9,11} & 0 \\ & & & & & & T & & & B_{10,10} & 0 & 0 \\ & & & & & & & R & & & B_{11,11} & 0 \\ & & & & & & & & Y & & & B_{12,12} \end{bmatrix} \cdot \begin{bmatrix} u_i \\ v_i \\ w_i \\ \varphi_{x,i} \\ \bar{\varphi}_{y,i} \\ \bar{\varphi}_{z,i} \\ u_j \\ v_j \\ w_j \\ \varphi_{x,j} \\ \bar{\varphi}_{y,j} \\ \bar{\varphi}_{z,j} \end{bmatrix} + \begin{bmatrix} F_1 \\ F_2 \\ F_3 \\ F_4 \\ F_5 \\ F_6 \\ F_7 \\ F_8 \\ F_9 \\ F_{10} \\ F_{11} \\ F_{12} \end{bmatrix}. \tag{25}$$

The local finite element matrix *B* in (25) consists formally of the linear stiffness matrix K_L and the linearized geometric stiffness matrix K_N (containing the terms with second order axial force N^{II} that has to be known or has to be evaluated by a linear elastic-static calculation) and the consistent mass matrix *M*:

$$\left[B\right] = \left[K_L + K_N - \omega^2 M\right]. \tag{26}$$

The terms B and F correspond to the previously derived terms of the local beam element matrices and load vectors in (6), (14), (17) and (24). In the modal analysis of a single straight beam the global finite element matrix coincides with the local matrix. For a general case, the global matrix of the beam and the beam structure are established in the usual finite element method way. In the modal and buckling analysis the eigenvalue problem is solved. In modal analysis, for given or calculated axial forces N^{II} and defined geometrical parameters and homogenized material properties and the global boundary conditions, the circular frequency ω is increased until the determinant of the global beam structure matrix tends to zero. This circular frequency is the natural circular frequency from which the natural frequency (eigenfrequency) can be calculated. In buckling analysis, the circular frequency ω is set to zero, and the second order beam theory axial force N^{II} is increased until the determinant of the global beam structure matrix tends to zero. Then, the axial force represents the buckling force N_{Ki}^{II}.Further, the mode or buckling shapes can be calculated by the transfer relations (5), (13), and (22). In static analysis, the circular frequency ω is set to zero and the load vector hast be established. The global and local displacements and rotations at the nodes are calculated from those the local internal forces and moments in the homogenized beam elements cross-sections are evaluated. After that the normal and shear stress is calculated in the beam cross sections with real distribution of material properties. The solution approach we have implemented into the software MATHEMATICA [21] by which the numerical calculations presented in the chapter 4 were done.

3 HOMOGENIZATION OF IN THREE DIRECTIONS VARYING MATERIAL PROPERTIES

One important goal of mechanics of heterogeneous materials is to derive their effective properties from the knowledge of the constitutive laws and complex micro-structural behavior of their components. Microscopic modeling expresses the relation between the characteristics of the components and the average (effective) properties of composites. In the case of FGM it is the relation between the characteristics of the components and the effective properties of FGM.

The methods based on homogenization theories (e.g. the mixture rules [22,23]; self-consistent methods [24]) have been designed and successfully applied to determine the effective material properties of heterogeneous materials from the corresponding material behavior of the constituents (and of the interfaces between them) and from the geometrical arrangement of the phases. In this context, the microstructure of the material under consideration is basically taken into account by a representative volume element (RVE).

Mixture rules are one of the methods for micromechanical modeling of heterogeneous materials. Extended mixture rules [25] are based on the assumption that the constituents volume fractions, formally denoted as fibers – f and matrix – m (the notation is very often used in the literature also for the FGM constituents, although this material is point wise isotropic and the reinforcing constituents are not of several forms and dimensions) vary continuously as polynomial functions, $v_f(x,y,z)$ and $v_m(x,y,z)$. The condition $v_f(x,y,z)+v_m(x,y,z)=1$ has to be fulfilled. The appropriated material property distribution in the real FGM beam (Figure 2a) then reads

$$p(x,y,z)=v_f(x,y,z)\,p_f(x,y,z)+v_m(x,y,z)\,p_m(x,y,z). \tag{27}$$

Here, $p_f(x,y,z)$ and $p_m(x,y,z)$ are the spatial distribution of material properties of the FGM constituents. The extended mixture rule (27) can be analogically used for FGM made of more than two constituents. The assumption of a polynomial variation of the constituent's volume fractions and material properties enables an easier establishing of the main field equations and allows the modeling of many common realizable variations.

In the research studies and in practical applications, the one directional variation of the FGM properties is mostly considered. For the FGM beams and shells the transversal variation (continuously or discontinuously, symmetrically or asymmetrically) has been mainly considered. There, an exponential law for variation of the constituents volume fractions through the beam's height is often presented, e.g. in [26-28] and in references therein. The homogenization of such variations is relatively simple. If the material properties vary only with respect to the longitudinal direction, the homogenization is frequently not needed since there are the FGM beam and link finite elements established that consider such variations in a very accurate and effective way [29-31]. The more complicated case is, when the material properties vary in three directions - namely in transversal, lateral and longitudinal directions of the FGM beam.

In this contribution, the homogenization techniques of spatially varying (continuously or discontinuously and symmetrically in transversal and lateral direction, and continuously in longitudinal direction) material properties of FGM beams of selected doubly-symmetric cross-sections are presented. The expressions are proposed for the evaluation of effective elastic modules for axial loading and for transversal and lateral bending complemented with the shear modules for transversal and lateral shear and uniform torsion and for themass density by the extended mixture rules (EMR) and the multilayer method (MLM).

Let us consider a two node straight beam element with predominantly rectangular cross-sectional area *A* (Figure 2). The composite material of this beam arises from mixing two constituents. The continuous polynomial spatial variation of the elastic modules and mass density can be caused by continuous polynomial spatial variation of both the volume fractions ($v_f(x,y,z)$ and $v_m(x,y,z)$) and the material properties ($p_f(x,y,z)$ and $p_m(x,y,z)$) of the FGM constituents.

In our case the elastic modulus $E(x,y,z)$, the Poisson ratio $\nu(x,y,z)$, and mass density $\rho(x,y,z)$ are calculated by expression (27). The FGM shear modulus is calculated by expression:

$$G(x,y,z)=\frac{E(x,y,z)}{2(1+\nu(x,y,z))} \tag{28}$$

If the Poisson's ratio of the constituents is approximately of the same value and the constituents volume fraction variation is not strong, then the FGM shear modulus can by calculated using a simplification

$$G(x,y,z)=\frac{E(x,y,z)}{\xi}, \tag{29}$$

where ξ is an average value of the function $\xi(x,y,z)=2(1+\nu(x,y,z))$

$$\xi=\frac{1}{L}\int_0^L\left(\frac{1}{A}\int_{(A)}\xi(x,y,z)dA\right)dx. \tag{30}$$

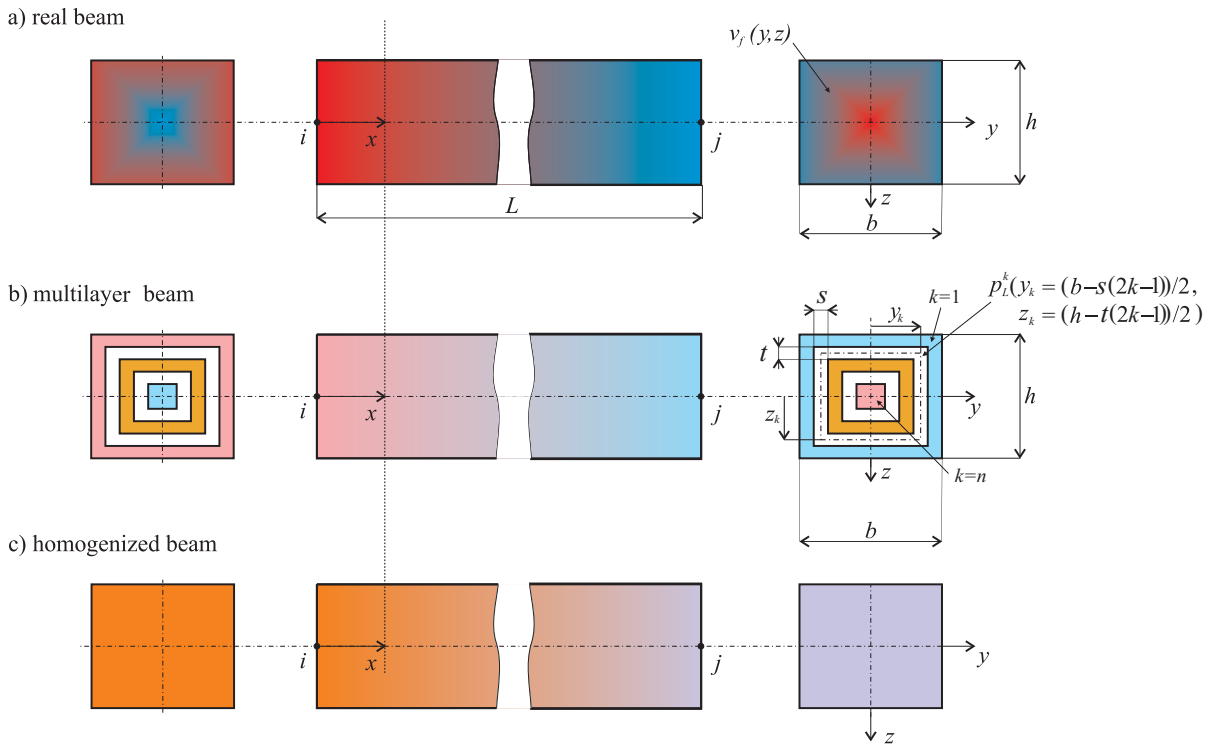

Figure 2: FGM beam with rectangular cross-section.

Homogenization of the spatially varying material properties (the reference volume is the volume of the whole beam) is done in two steps. In the first step, the real beam (Figure 2a) is transformed into a multilayer beam (Figure 2b). Homogenized material properties of the layers are calculated with the EMR [30]. Competent homogenized layer *k* at position *x* has a constant volume fractions and the material properties of the constituents in the *y* and *z* direction. They are calculated as an average value from their values at the boundaries of the respective layer. Polynomial variation of these parameters appears with respect to the longitudinal direction of the layer. Sufficient accuracy of the proposed substitution of the continuous transversal and lateral variation of material properties by the layer-wise constant distribution of material properties is reached if the division to layers is fine enough. In the second step, the effective longitudinal material properties of the homogenized beam are derived using the MLM. These homogenized material properties are constant through the beam's height and depth but they vary continuously along the longitudinal beam axis. Accordingly, the beam finite element equations are established for the homogenized beam (Figure 2c) in order to calculate the primary effective beam unknowns (the displacements, temperatures, electric potential, eigenfrequency, buckling force, etc…). The secondary variables, for example the mechanical stress, have to be calculated from the internal local forces and moments on the real beam [29].

The homogenized elastic modules for tension-compression - $E_L^{NH}(x)$, bending about axis *y* - $E_L^{M_yH}(x)$, bending about axis *z* - $E_L^{M_zH}(x)$, shear in *y* direction - $G_{Ly}^{H}(x)$, shear in *z* direction - $G_{Lz}^{H}(x)$, torsion $G_L^{M_xH}(x)$, and the homogenized mass density for axial loading $\rho_L^{NH}(x)$ and torsion $\rho_L^{M_xH}(x)$ can be calculated using the following expressions:

$$E_L^{NH}(x)=\frac{\sum_{k=1}^{n}E_k(x)A_k}{A},\quad E_L^{M_yH}(x)=\frac{\sum_{k=1}^{n}E_k(x)I_{y,k}}{I_y},\quad E_L^{M_zH}(x)=\frac{\sum_{k=1}^{n}E_k(x)I_{z,k}}{I_z},\tag{31}$$

$$G_{Ly}^{H}(x)=\frac{\sum_{k=1}^{n}k_{y,k}^{sm}G_k(x)A_k}{k_y^{sm}A},\quad G_{Lz}^{H}(x)=\frac{\sum_{k=1}^{n}k_{z,k}^{sm}G_k(x)A_k}{k_z^{sm}A},\tag{32}$$

$$G_L^{M_xH}(x)=\frac{\sum_{k=1}^{n}G_k(x)I_{T,k}}{I_T},\quad \rho_L^{NH}(x)=\frac{\sum_{k=1}^{n}\rho_k(x)A_k}{A},\ \rho_L^{M_xH}(x)=\frac{\sum_{k=1}^{n}\rho_k(x)I_{p,k}}{I_p}.\tag{33}$$

Here, A_k denotes the cross-sections area, $E_k(x)$is the elastic modulus, $I_{y,k}$ and $I_{z,k}$ are the second moments of area, $G_k(x)$ is the shear modulus, $I_{T,k}$ is the torsion constant and $\rho_k(x)$ is the mass density, $I_{p,k}$ is the polar moment of area of the kth layer. The exact expressions for homogenization of spatial varying (continuously or discontinuously and symmetrically in transversal and lateral direction, and continuously in longitudinal direction) material properties for the FGM beams depend on the form of the cross-section. For rectangular hollow cross-sections we present the corresponding expressions in the following chapters.

3.1 Hollow cross-section

A straight beam of hollow cross-sectional area $A=b_1h_1-b_nh_n$(Figure 3) is made of a FGM whose properties vary in the y and z direction continuously and symmetrically according the main inertial planes, $x-y$ and $x-z$, and continuously in longitudinal beam direction x. Further, $I_y=\frac{b_1h_1^{\,3}}{12}-\frac{b_nh_n^{\,3}}{12}$ and $I_z=\frac{h_1b_1^{\,3}}{12}-\frac{h_nb_n^{\,3}}{12}$ are the second moments of area, $I_p=I_y+I_z$ is the polar moment of area, $\overline{A}_y=k_y^{sm}A$ and $\overline{A}_z=k_z^{sm}A$ refer to the reduced cross-sectional areas – by the average shear correction factors k_y^{sm} and k_z^{sm} [17,32,75], and $I_T=\frac{2(h_1-t)^2(b_1-s)^2}{\frac{h_1-t}{s}+\frac{b_1-s}{t}}$ is the torsion constant. Here, s and t refer to the thicknesses of the cross-section walls.

For the homogenization of spatially varying material properties the hollow cross-sectional area is divided into n hollow parts, where $t_k=(h_1-h_n)/2n$ is the flange thickness and $s_k=(b_1-b_n)/2n$ is the web thickness (Figure 3), respectively. The hollow area of the kth part $(k\in\langle 1,\ n\rangle)$ is: $A_k=2t_k(b_1-s_k(2k-1))+2s_k(h_1-t_k(2k-1))$. The second moments of area of the kth part are: $I_{y,k}=(b_1-s_k(2k-2))(h_1-t_k(2k-2))^3/12-(b_1-2ks_k)(h-2kt_k)^3/12$, $I_{z,k}=(b_1-s_k(2k-2))^3(h_1-t_k(2k-2))/12-(b_1-2ks_k)^3(h_1-2kt_k)/12$ .The polar moment of area of kth part is $I_{p,k}=I_{y,k}+I_{z,k}$.

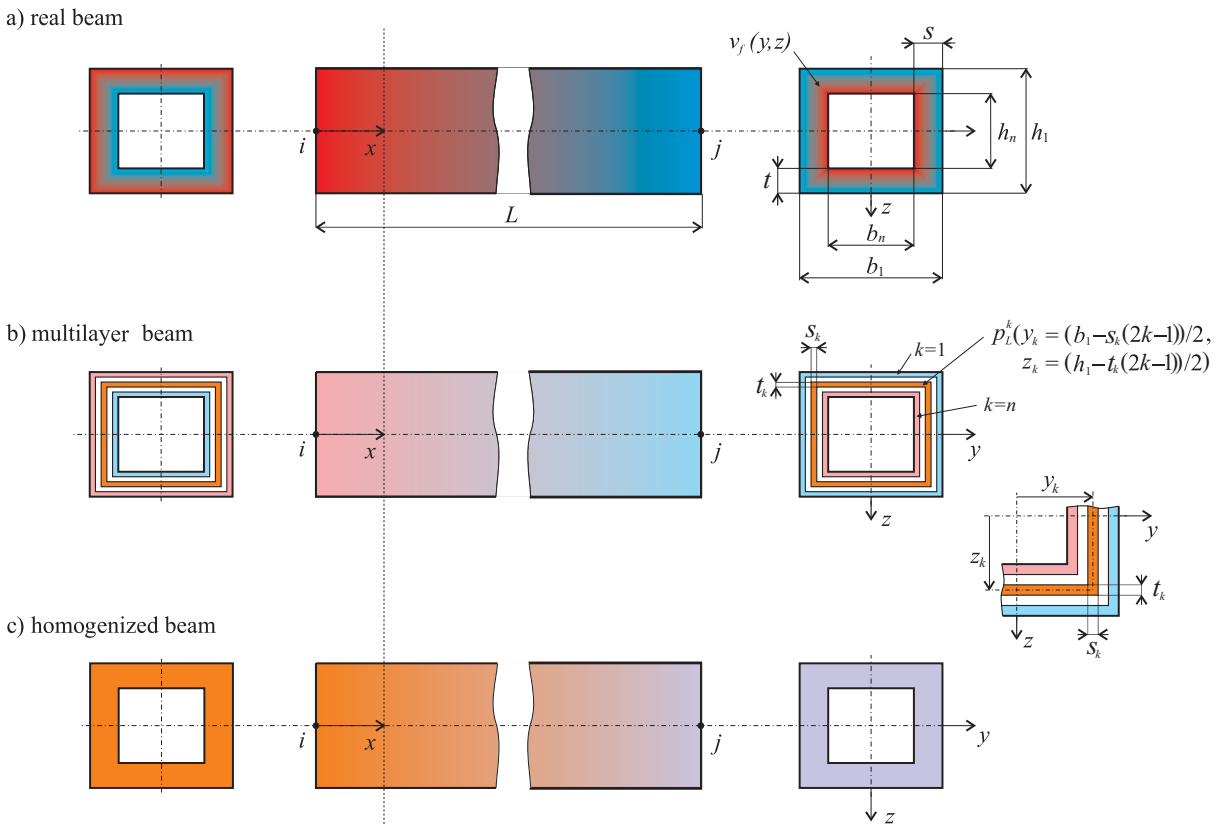

Figure 3: A straight FGM beam of hollow cross-section.

According to (27) and (28) the real material properties are: $E(x,y,z)$ is the elastic modulus, $\nu(x,y,z)$ is the Poisson's ratio, $G(x,y,z)=E(x,y,z)/(2(1+\nu(x,y,z)))$ is the shear modulus and $\rho(x,y,z)$ is the mass density: $(x\in<0,L>, y\in<\pm h_n/2, \pm h_1/2>, z\in<\pm b_n/2, \pm b_1/2>)$.
The effective homogenized material properties, like the elastic modules, are calculated under assumption, that the relevant stiffness of the homogenized beam is equal to the stiffness of the real beam virtually divided on the hollow parts. Thus, we get the effective elastic modulus for axial loading

$$E_L^{NH}(x)=\frac{\sum_{k=1}^{n-1}E_k(x)A_k}{A}, \tag{34}$$

with $E_k(x)=\left[E(x,y,z)\right]_{\substack{y=y_k\\z=z_k}}$ and the effective elastic modules for bending about the y and z axis,

$$E_L^{M_yH}(x)=\frac{\sum_{k=1}^{n}E_k(x)I_{y,k}}{I_y},\quad E_L^{M_zH}(x)=\frac{\sum_{k=1}^{n}E_k(x)I_{z,k}}{I_z}. \tag{35}$$

The effective elastic modulus for uniform torsion reads,

$$G_L^{M_xH}(x)=\frac{\sum_{k=1}^{n}G_k(x)I_{T,k}}{I_T}, \tag{36}$$

with $G_k(x) = \left[G(x,y,z)\right]_{\substack{y=y_k \\ z=z_k}}$. The torsion constant of the kth hollow part $\left(k \in \langle 1,\ n \rangle\right)$ can be evaluated as

$$I_{T,k} = \frac{2\left(b_1 - s_k(2k-1)\right)^2 \left(h_1 - t_k(2k-1)\right)^2}{\dfrac{\left(b_1 - s_k(2k-1)\right)}{t_k} + \dfrac{\left(h_1 - t_k(2k-1)\right)}{s_k}}. \tag{37}$$

The effective shear modulus in y direction is given by,

$$G_{Ly}^{H}(x) = \frac{\sum_{i=1}^{n} k_{y,k}^{sm} G_k(x) A_k}{k_y^{sm} A}, \tag{38}$$

with the average shear correction factors: k_y^{sm} for whole rectangular cross-section and $k_{y,k}^{sm}$ for kth part.
The shear modulus in z direction then reads,

$$G_{Lz}^{H}(x) = \frac{\sum_{k=1}^{n} k_{z,k}^{sm} G_k(x) A_k}{k_z^{sm} A}, \tag{39}$$

with the average shear correction factors: k_z^{sm} for whole rectangular cross-section and $k_{z,k}^{sm}$ for kth part.
The effective mass density for tension - $\rho_L^{NH}(x)$ and torsion $\rho_L^{M_xH}(x)$ is

$$\rho_L^{H}(x) = \frac{\sum_{k=1}^{n} \rho_k(x) A_k}{A}, \qquad \rho_L^{M_xH}(x) = \frac{\sum_{k=1}^{n} \rho_k(x) I_{p,k}}{I_p}, \tag{40}$$

with $\rho_k(x) = \left[\rho(x,y,z)\right]_{\substack{y=y_k \\ z=z_k}}$.It should be noted, that the effective mass density for tension has been taken also for the lateral and transversal bending.

4 NUMERICAL INVESTIGATIONS

4.1 Example 1: FGM beam structure - hollow cross-section

The FGM beam structure with a constant rectangular hollow cross-section is considered (Figure 4), which consists of two parts – Beam1 and Beam2. Its geometry is given byh_1 = 0.005 m, h_n = 0.00375 m, b_1 = 0.01 m, b_n = 0.0075 m and L = 0.1 m. The angle between the beams is $\theta = 150°$. The cross-sectional area is $A = 2.1875\times10^{-5}$ m^2, the second moments of area are $I_{y'} = 7.12077\times10^{-11}$ m^4 and $I_{z'} = 2.84831\times10^{-10}$ m^4, the polar moment of area is $I_p = I_{y'} + I_{z'} = 3.56038\times10^{-10}$ m^4 and the torsion constant is $I_T = 1.6748\times10^{-10}$ m^4.

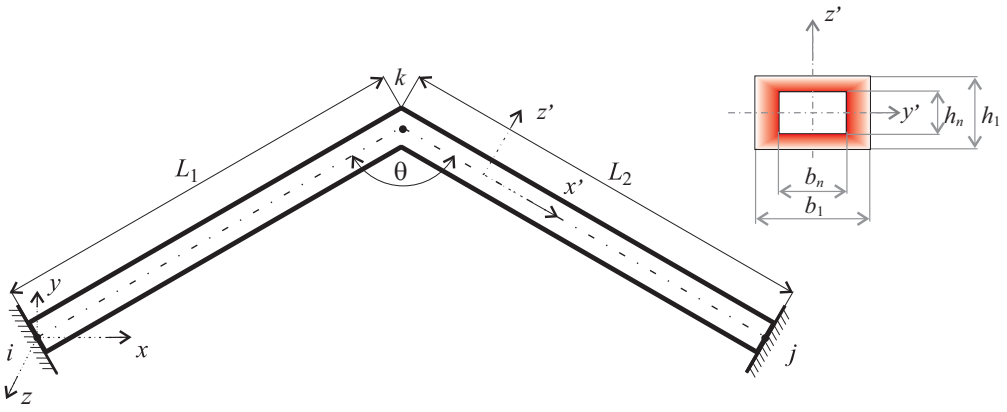

Figure 4: FGM beam structure in global (*x*, *y*, *z*) coordinate system.

The material of the beam consists of two components: Aluminum Al6061-TO – denoted with index *m* and Titanium carbide TiC – denoted with index *f*. The material properties of the components are assumed to be constant and their values are: Aluminum Al6061-TO – the elasticity modulus $E_m = 69.0\,\text{GPa}$, the mass density $\rho_m = 2700$ kgm^{-3}, the Poisson's ratio $\nu_m = 0.33$; Titanium carbide TiC – the elasticity modulus $E_f = 480.0\,\text{GPa}$, the mass density $\rho_f = 4920$ kgm^{-3}, the Poisson's ratio $\nu_f = 0.20$.

The TiC volume fraction varies in the local y' and z' direction linearly and symmetrically according to the $x'-y'$ and $x'-z'$ planes: $\left[v_f\left(y',z'\right)\right]_{\substack{y'=\pm h_n/2\\ z'=\pm b_n/2}} = 0$, $\left[v_f\left(y',z'\right)\right]_{\substack{y'=\pm h_1/2\\ z'=\pm b_1/2}} = 1$ - the inner edges of the cross-sectional area are made of pure Al6061-TO –and the outer cross-section edges are made of pure TiC. Constant effective material properties are considered in the local x' – direction of both beams. Using EMR and MLM the effective elastic modulus (in [GPa]) for axial loading E_L^{NH}, for bending about axis y' - $E_L^{M_yH}$ and about axis z' - $E_L^{M_zH}$ the shear moduli G_{Ly}^H and G_{Lz}^H, the torsional shear modulus $G_L^{M_xH}$, and the mass density ρ_L^{NH} [kgm^{-3}] for tension and $\rho_L^{M_xH}$ [kgm^{-3}] for torsion have been calculated by equations (34 - 40). The influence of the number of divisions *n* to the layers on the homogenized material properties [32, 33] is shown in Table 1. The average shear correction factors k_y^{sm} and k_z^{sm} for $n = 20$ layers are $k_y^{sm} = 0.4712$ and $k_z^{sm} = 0.2910$ [32, 33]. For homogeneous hollow cross-section, following shear correction factors are obtained: $k_y = 0.5081$ and $k_z = 0.3291$ (calculated e.g. with ANSYS [34], for rectangular hollow beam-section).

layers *n*	E_L^{NH}	$E_L^{M_yH} = E_L^{M_zH}$	$G_{Ly}^H = G_{Lz}^H$	$G_L^{M_xH}$	ρ_L^{NH}	$\rho_L^{M_xH}$
2	281.839	296.151	112.716	120.614	3849.643	3926.946
5	283.894	302.229	113.901	124.066	3860.743	3959.777
10	284.188	303.098	114.071	124.561	3862.328	3964.469
15	284.242	303.259	114.102	124.653	3862.222	3965.339
20	284.261	303.315	114.113	124.685	3862.725	3965.643

Table 1: Influence of the number of division *n* to the layers on the homogenized material properties.

Modal analysis

The FGM beam structure, clamped at the node *i* and *j*, is studied by modal analysis. The effect of axial force is not considered by this example. The first six eigenfrequencies *f* [Hz] are given in Table 2 using the new FGM beam finite element (NFE) and homogenized material properties for $n = 20$. Only two of our proposed FGM finite element are used – one for each part. For comparison purposes, the same problem is solved using a very fine mesh – 21600 of SOLID186 elements of the FEM program ANSYS [34]. The average relative difference Δ[%] between eigenfrequencies calculated by our method (NFE) and the ANSYS solution is evaluated.

eigenfrequencies *f* [Hz]		NFE without shear	NFE with shear	ANSYS	Δ[%] without shear	Δ[%] with shear
1st	flexural – *xz* plane	2392.0	2361.1	2343.6	2.07	0.75
2nd	flexural – *xy* plane	3859.1	3765.4	3798.8	1.65	0.82
3rd	flexural – *xy* plane	4444.0	4384.0	4341.1	2.37	0.99
4th	flexural – *xz* plane	7391.0	7123.3	7182.5	2.96	0.77
5th	flexural – *xy* plane	9147.1	9027.1	8928.4	2.57	1.23
6th	torsional	10051.1	10013.4	9896.8	1.56	1.18

Table 2: Eigenfrequencies of the FGM beam structure.

A comparison of 1st,2nd and 3rd eigenforms of the FGM beam structure evaluated by the new FGM beam finite element and FEM program ANSYS is shown in Figures 5 - 7.

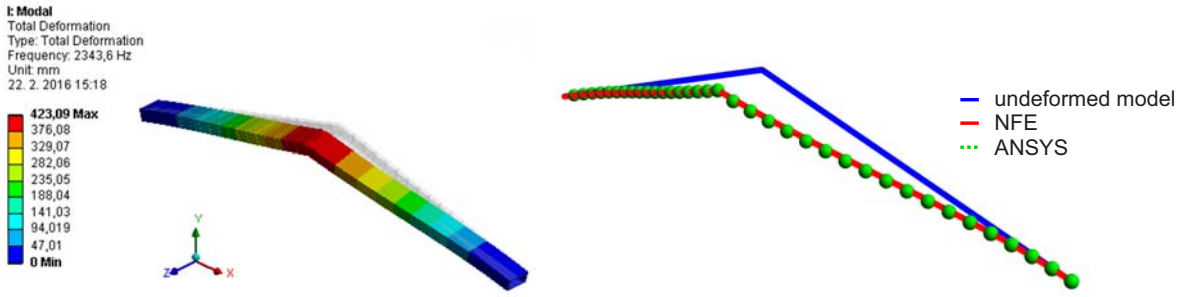

Figure 5: The 1st eigenform of the FGM beam structure displayed by the ANSYS postprocessor and comparison of NFE and ANSYS.

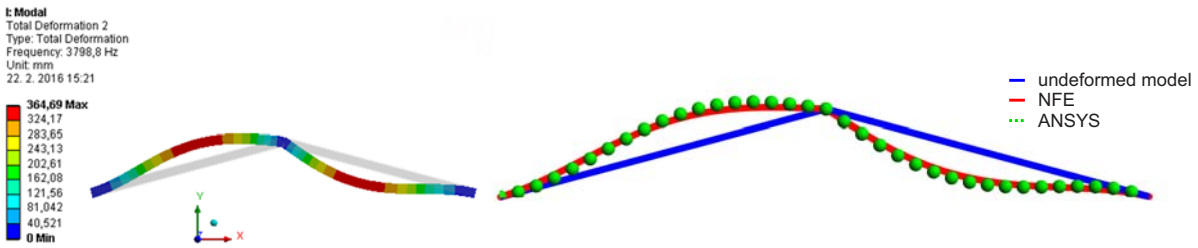

Figure 6: The 2nd eigenform of the FGM beam structure displayed by the ANSYS postprocessor and comparison of NFE and ANSYS.

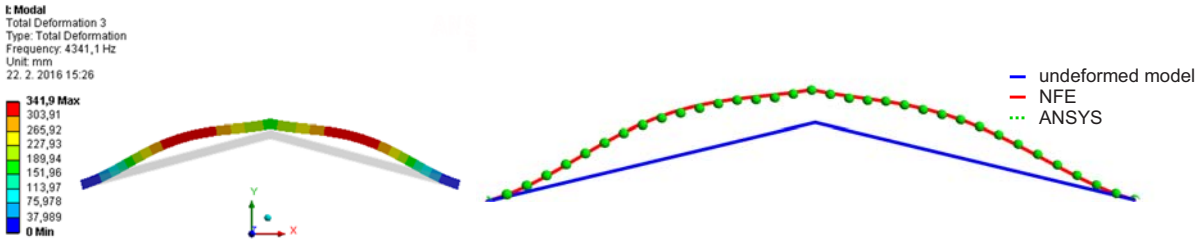

Figure 7: The 3rd eigenforms of the FGM beam structure displayed by the ANSYS postprocessor and comparison of NFE and ANSYS.

Elasto-static analysis

The FGM beam structure, clamped at the node *i* and *j*, loaded by the vertical force $F_{ky} = 100$ N in the global negative *y* direction and the torsion moment $M_{kx} = 100$ Nm about global *x*-axis at point *k*, is studied by elasto-static analysis. The effects of axial forces is not considered by this example. The displacements according the global coordinate system at the point *k* are given in Table 3 using the new FGM beam finite element (NFE) and homogenized material properties for *n* = 20. Only two of the herein proposed new FGM finite elements were used – one for each part. For comparison purposes, the same problem is solved using a very fine mesh – 21600 of SOLID186 elements of the FEM program ANSYS [34]. The average relative difference Δ[%] between displacements calculated by our method and the ANSYS solution is evaluated.

Displacements [mm], [rad]	NFE without shear correction	NFE with shear correction	ANSYS	Δ[%] without shear correction	Δ[%] with shear correction
v_k	-0.01135	-0.01137	-0.01140	0.39	0.27
w_k	-2.56285	-2.56285	-2.58651	0.91	0.91
φ_{xk}	0.19804	0.19804	0.20030	1.13	1.13

Table 3: Global displacements at point *k*.

The total deformation of the FGM beam structure is shown in Figure 8.

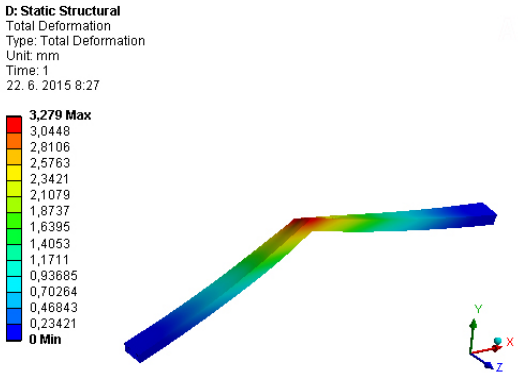

Figure 8: Total deformation of the FGM beam structure.

As can be seen in Table 4, a very good agreement of our results is obtained.

4.2 Example 2: FGM beam – spatial variation of material properties

The cantilever FGM beam on varying horizontal and vertical Winkler foundation is considered (as shown in Figure 9). Its rectangular cross-section is constant with height h = 0.005 m and width b = 0.01 m. The length of the beam is L = 0.1 m.

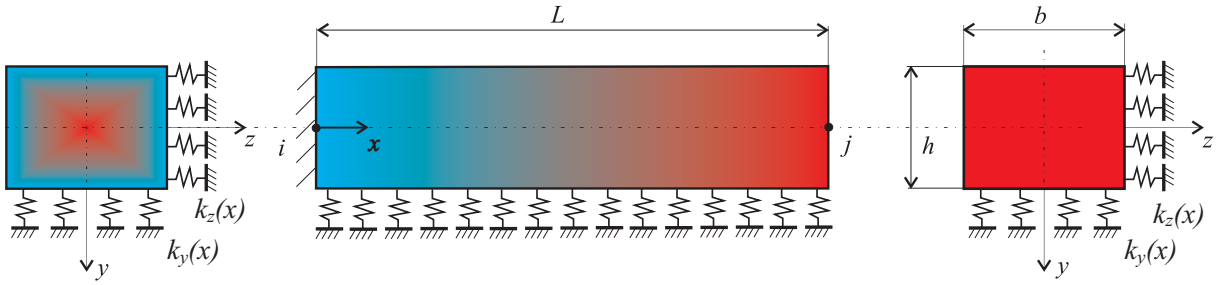

Figure 9: Clamped beam on elastic foundation with spatially varying material properties.

The beam is made of a mixture of two components: Aluminum Al6061-TO and Titanium Carbide TiC, their constant constituent's material properties are given in Case I. The Aluminum volume fraction, in this case, varies linearly and symmetrically according to the $x-y$ and $x-z$ planes: At node i is $\left\lfloor v_{fi}(y,z)\right\rfloor_{\substack{y=0\\z=0}}=1, \left\lfloor v_{fi}(y,z)\right\rfloor_{\substack{y=\pm h/2\\z=\pm b/2}}=0$ and then vary continuous linearly in the longitudinal direction to the constant value at node j ($v_{fj}=1$).

Using EMR and MLM with n = 20 layers the effective elastic modulus for axial loading E_L^{NH}, for bending about axis y - $E_L^{M_yH}$ and about axis z - $E_L^{M_zH}$, shear modules G_{Ly}^{H} and G_{Lz}^{H}, torsional shear modulus $G_L^{M_xH}$, and mass density ρ_L^{NH} for tension and $\rho_L^{M_xH}$ for torsion are evaluated as:

$$E_L^{NH}=342.109-2731.095x \text{ GPa};$$

$$E_L^{M_yH}=E_L^{M_zH}=396.429-3274.293x \text{ GPa};$$

$$G_{Ly}^{H}=G_{Lz}^{H}=138.581-1129.418x \text{ GPa};$$

$$G_L^{M_xH}=162.233-1362.936x \text{ GPa};$$

$$\rho_L^{NH}=4175.19-14751.9x \text{ kgm}^{-3};$$

$$\rho_L^{M_xH}=4468.34-17683.43x \text{ kgm}^{-3}.$$

Modal analysis

The FGM cantilever beam, clamped at the node i, and resting on varying Winkler elastic foundation $k_y(x)$=5000-30000x+60000x^2 kN/m^2 and $k_z(x)$=5000-1000x+6000x^2 kN/m^2 is studied by modal analysis. The average shear correction factors in y' – direction $k_y^{sm}=5/6$ and in z' – direction $k_z^{sm}=5/6$ are used [35]. The first nine eigenfrequencies f [Hz] are evaluated as shown in Table 4. It is use only one of our proposed finite element. The effect of axial force was not considered in this example. The same problem is solved using a very fine mesh – 32000 of SOLID186 elements of the FEM program ANSYS [34]. The results of ANSYS as

well as the results of the NFE are presented in Table 4. The average relative difference Δ[%] between eigenfrequencies calculated by our method and the ANSYS solution is evaluated.

eigenfrequencies f [Hz]		NFE without foundation	ANSYS without foundation	Δ[%]	NFE with foundation	ANSYS with foundation	Δ[%]
1st	flexural - axis y	838.9	844.9	0.71	1356.1	1365.3	0.67
2nd	flexural - axis z	1660.0	1674.4	0.86	1896.3	1911.3	0.78
3rd	flexural - axis y	4329.5	4301.7	0.65	4433.4	4413.5	0.45
4th	flexural - axis z	8288.5	8228.8	0.73	8332.2	8275.1	0.69
5th	flexural - axis y	11046.0	10920.0	1.15	11125.8	10961.0	1.50
6th	torsional	11182.0	10926.0	2.34	11048.0	10969.0	0.72
7th	flexural - axis z	20023.0	19907.0	0.58	20051.0	19925.0	0.63
8th	flexural - axis y	20379.0	20312.0	0.33	20397.1	20333.0	0.32
9th	axial	22212.6	22213.0	0.01	22212.7	22213.0	0.01

Table 4: Eigenfrequencies of the FGM beam with and without elastic foundation.

Again, a very good agreement of our results compared to ANSYS is indicated in Table 4. For instance, the 1st, 6th and 9th mode of the FGM beam structure displayed by ANSYS is shown in Figure 10.

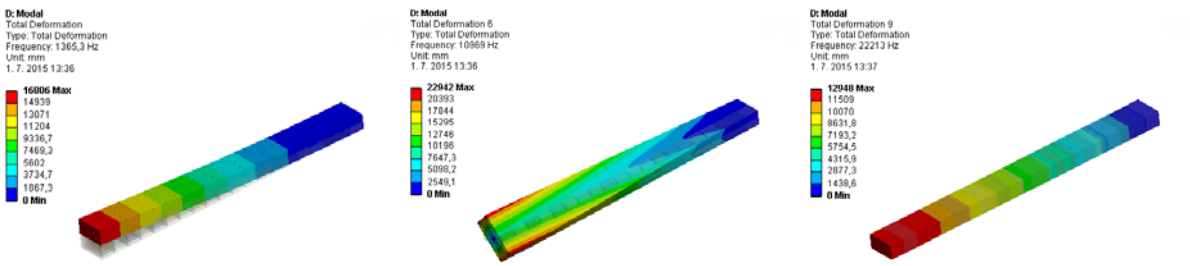

Figure 10: The 1th and 6th and 9th eigenforms of the beam (with Winkler elastic foundations).

Buckling and elastic-static analysis

The FGM cantilever beam, clamped at the node i, has been studied by buckling and elastic-static analysis. All the calculations were done with our 3D FGM beam finite element (NFE) which we have implemented into the code MATHEMATICA [21]. Additionally, the effect of axial force was considered. It has to be pointed out that the entire structure is discretized using only one herein proposed finite element.

The critical buckling force calculated by our 3D FGM beam finite element is $N_{Ki}^{II} = 7.171$ kN and calculated by ANSYS (with 50 of BEAM188 elements) is $N_{Ki}^{II} = 7.081$kN. The first buckling form is shown in Figure 11. In the elasto-static analysis the axial force $N^{II} \equiv N$ have been chosen as a part of the critical buckling force N_{Ki}^{II}.

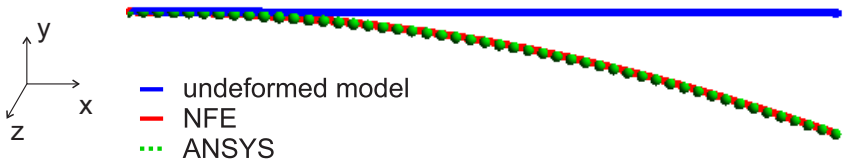

Figure 11: The first buckling form.

In the elastic-static analysis, the cantilever FGM beam resting on varying vertical Winkler elastic foundation $k_y = 5000 - 30000x + 600000x^2$ kN/m^2 is loaded by forces $F_y = F_z = 50$ N and $F_x = -2$ kN at node j (Figure 12). The average shear correction factors in y' – direction $k_y^{sm} = 5/6$ and in z' – direction $k_z^{sm} = 5/6$ are used [35]. The displacements at node j are evaluated using the only one new FGM beam finite element (NFE). The same problem is solved using a very fine mesh – 23015 of SOLID186 elements of the FEM program ANSYS [34]. The results of ANSYS as well as the results of the NFE are presented in Table 5. The average relative difference Δ[%] between displacements calculated by our method and the ANSYS solution is evaluated.

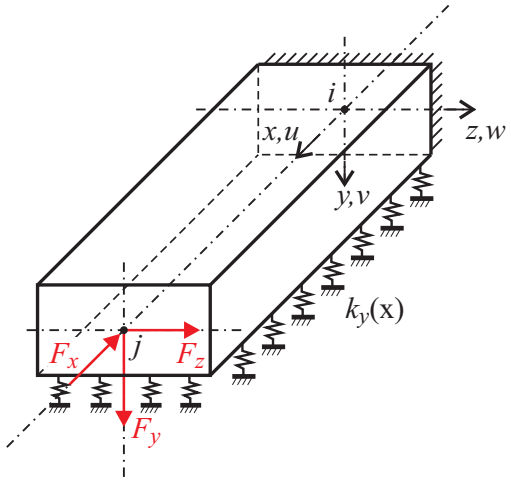

Figure 12: Loaded FGM beam.

Displacements at node j [mm], [rad]	NFE with foundation	ANSYS with foundation	NFE without foundation	ANSYS without foundation
u_j	-0.02445	-0.02507	-0.02445	0.02507
v_j	0.24641	0.24933	0.74414	0.75348
w_j	0.14452	0.14791	0.14452	0.14791
φ_{yj}	-0.00247	-0.00256	-0.00247	-0.00256
φ_{zj}	0.00503	0.00527	0.1304	0.01321

Table 5: Displacements at node j with and without elastic foundation.

The comparison of the vertical beam deflection curve with and without elastic foundation is shown in Figure 13.

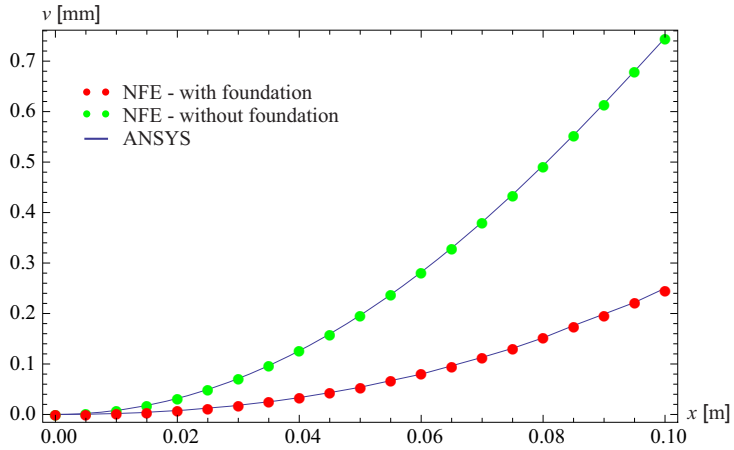

Figure 13: Vertical beam deflection curve with and without elastic foundation.

The bending moments about the y and z – axis for case without elastic foundation are shown in Figures 14 and 15, respectively. The Figures 16 and 17 show the transversal force in y and z – axis. The comparison of the bending moments $M_y(x=0)$, $M_z(x=0)$ and transversal forces $R_y(x=L)$, $R_{yz}(x=L)$ for the case F_x = -2 kN calculated by our approach and by ANSYS are compared in Table 6.

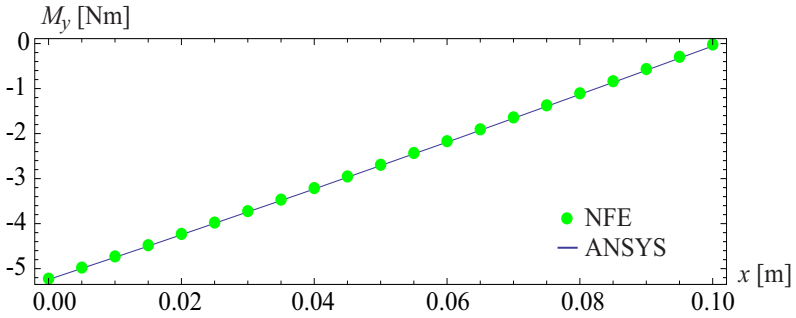

Figure 14: Bending moment about the y – axis (without elastic foundation).

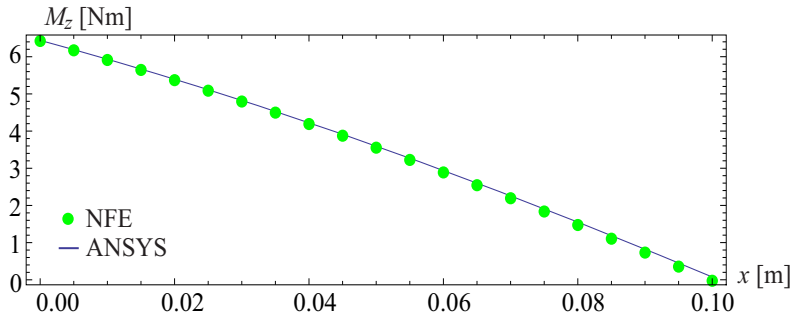

Figure 15: Bending moment about the z – axis (without elastic foundation).

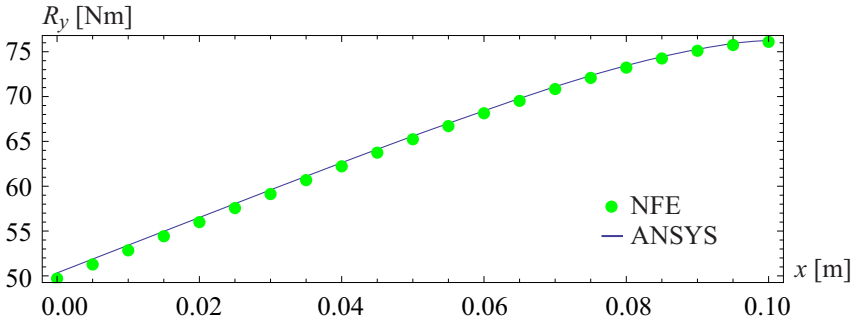

Figure 16: Transversal force in y – axis (without elastic foundation).

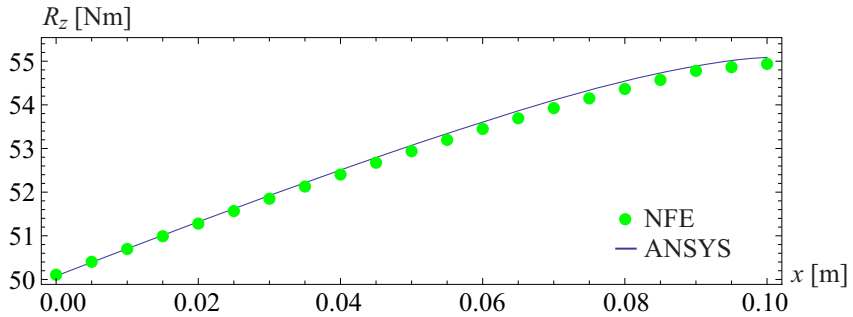

Figure 17: Transversal force in z – axis (without elastic foundation).

	NFE Fx = -2 kN	ANSYS Fx = -2 kN	Δ[%]
$M_y(x=0)$ [Nm]	-5.2182	-5.2416	0.45
$M_z(x=0)$ [Nm]	6.4691	6.4404	0.45
$R_y(x=L)$ [N]	54.9472	55.0873	0.25
$R_z(x=L)$ [N]	76.2088	76.2251	0.02

Table 6: Bending moments and transversal forces.

In Figure 18, the resultant normal stress, caused by axial, transversal and lateral forces, in the clamped cross-section is shown that was calculated by our approach [18] extended here for variation of material properties in three directions.

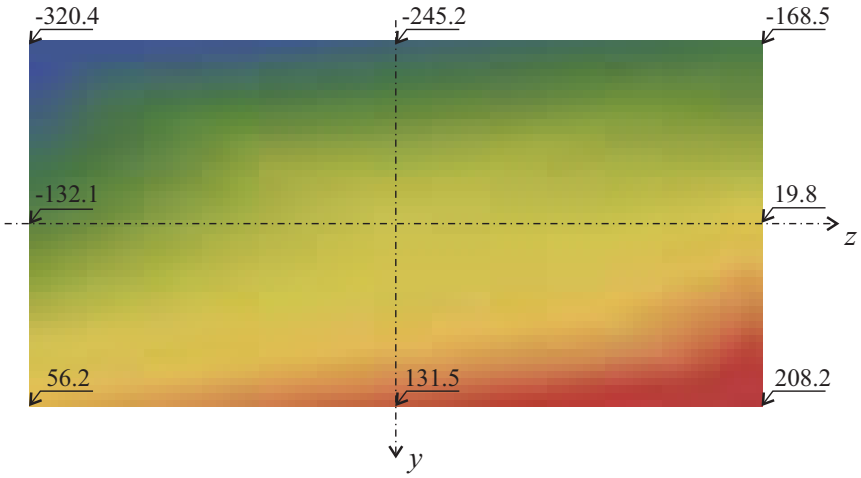

Figure 18: Resultant normal stress $\sigma(x, y, z)$ [MPa] at position $x = 0$ calculated by our approach [18].

In Figure 19, the resultant normal stress, caused by axial, transversal and lateral forces, in the clamped cross-section is shown that was calculated by ANSYS (using a very fine mesh – 23015 of SOLID186). As can be seen, a very good agreement of both solution method has been obtained at all marked points excluding the corners. As is well known, the solutions with 3D solid finite elements produce in the sharp corners incorrect stress first of all by the very fine meshes. In the nearby points of the sharp corners is the match of the results very good (see the details in Figure 19). More detailed description of the stress calculation for the FGM beam with spatial variation of material properties will be given in our newly prepared paper.

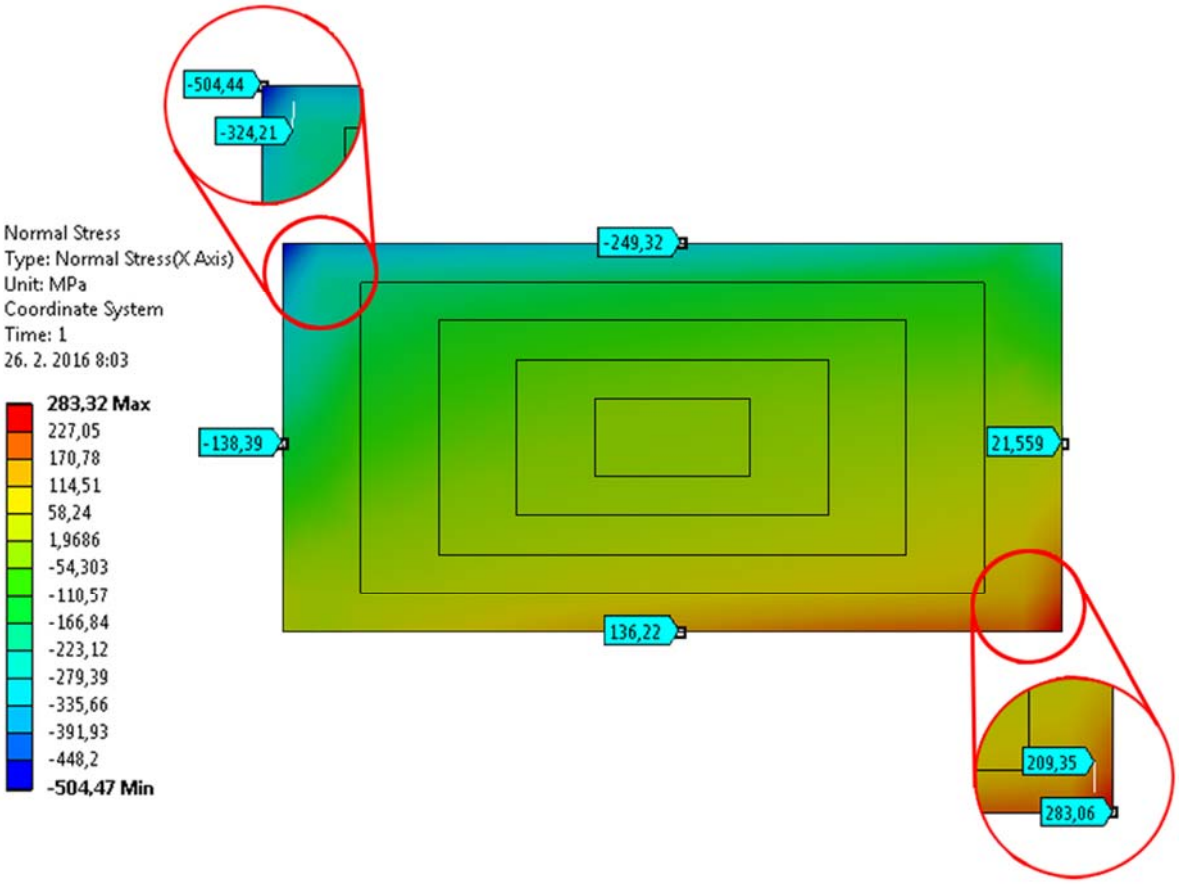

Figure 19: Normal stress $\sigma(x, y, z)$ [MPa] at position $x = 0$ calculated by ANSYS (SOLID186)

5 CONCLUSION

On base of the transfer relations for the 3D straight FGM beam of doubly symmetric cross-section with longitudinal polynomial variation of the effective material properties, the effective matrix of the 3D beam finite element for static, modal and buckling analysis of the FGM single beams and beam structures is established in this contribution. Symmetrically transversal and lateral, and continuously longitudinal variation of material properties is considered in the real beam. Homogenization of the spatially varying material properties in the real FGM beam and the calculation of effective parameters of the homogenized beam are done by the extended mixture rules and the multilayer method (MLM). Effects of the varying planar Winkler elastic foundations and the shear force deformation (by means of the average shear correction factors) and the consistent mass and mass moment of inertia distribution are

taken into account. The effect of axial force is included for the flexural deformations as well that allows performing of analysis within the 2nd order beam theory. All the derived equations were programmed through the software MATHEMATICA [21] and the numerical calculations were carried out. In modal and buckling analysis, the eigenvalue problem is solved. In buckling analysis, the circular frequency ω is set to zero and axial force N is increased the determinant of the global matrix of the beam structure tends to zero. This axial force corresponds to the critical buckling force. In modal analysis, for given internal axial forces N in the competent beams and geometrical parameters and material and boundary conditions, the circular frequency ω is increased until the determinant of the global matrix of the beam structure tends to zero. This circular frequency corresponds to the natural circular frequency from which the natural frequency (eigenfrequency) is calculated. In linearized elastostatic analysis (according the second order beam theory), the internal axial forces have to be evaluated that input in the linearized geometric stiffness matrix. By the linear beam theory only linear stiffness matrix is established. The load vector is established and the local and global displacements and internal forces are calculated. After that, as usually, the secondary variables like eigen- and buckling- forms, and the stress are calculated. The main issue of numerical investigations is the modal, buckling and elastostatic analysis of FGM beam structures (single beams and spatial beam structures) with spatial variation of material properties. By selected numerical examples the effect of axial and shear forces is evaluated. The results carried out by our approach are compared with results obtained using very fine beam and continuum meshes in the FEM program ANSYS [34]. An excellent agreement of our solution results is obtained, which confirms respectable accuracy and effectiveness of our approach.

The main advantage of the new beam finite element is that the individual beams of the beam structure with spatial variation of material properties (continuous or layered but symmetrically in transversal and lateral direction, and continuous polynomial in longitudinal direction) can be modeled with only one beam finite element, because the variation of the material properties is relatively accurately included into the finite element matrix. Another advantage is that the beam finite element can be very effectively used also for the modeling of spatial beam structures.

Disadvantage of this approach is that by more complicated variation of material properties some problems arise by the transfer constants calculation. This problem can be solved by the dividing of the definition domain of the transfer functions [20]. Another problems comparing to continuum approach can arise by the beams with complex cross-sectional area.

Acknowledgement: This work was financially supported by grants of Science and Technology Assistance Agency no. APVV-0246-12 and Scientific Grant Agency of the Ministry of Education of Slovak Republic and the Slovak Academy of Sciences and VEGA No. 1/0453/15.

REFERENCES

[1] F. Ebrahimi, E. Salari, Size-dependent free flexural vibrational behavior of functionally graded nanobeams using semi-analytical differential method. *Composite Part B,* **79**: 156-169, 2015.

[2] F. Ebrahimi, E. Salari, Nonlocal thermo-mechanical vibration analysis of functionally graded nanobeams in thermal enviroment. *ActaAstronautika*; **113**: 29-50, 2015.

[3] S.E. Ghiasian, Y. Kiani, M.R. Eslami, Nonlinear thermal dynamic buckling of FGM beams. *European Journal of Mechanics A/Solids*, **54**: 232-242, 2015.

[4] U. Eroglu, In-plane free vibration of circular beams made of functionally graded material in thermal environment: Beam theory. *Composite Structures*, **122**: 217-228, 2015.

[5] M. Meradjah, A. Kaci, M.S.A. Houari, A. Tounsi, S.R. Mahmoud, A new higher order shear and normal theory of fuctionaly graded beams. *Steel and Composite Structures*, **18**: 793-809, 2015.

[6] N. Wattanasakulpong, Q. Mao, Dynamic response of Timoshenko fuctionally graded beams with classical and non-classical boundary conditions using Chebyshev collocation method. *Composite Structures*, **119**: 346-354, 2015.

[7] R. Bennai, H.A. Atmane, A. Tounsi, A new higher-order shear and normal deformation theory for functionally graded sandwich beams. *Steel and Composite Structures*, **19**: 521-546, 2015.

[8] S. El-Borgi, R. Fernandes, J.N. Reddy, Non-local free and forced vibrations of graded nanobeams resting on a non-linear elastic foundation. *Int. J. of Non-Linear Mechanics*, **77**: 348-363, 2015.

[9] I.C. Dikaros, E.J. Sapountzakis, Non-uniform shear warping effect in the analysis of composite beams by BEM. *Engineering Structures*, **76**: 215 – 234, 2014.

[10] I.C. Dikaros, E.J. Sapountzakis, Generalized warping analysis of composite beams of an arbitrary cross-section by BEM. I: Theoretical considerations and numerical implementation. *Engineering Mechanics* 2014; DOI: 10.1061/(ASCE) EM.1943-7889.0000775.

[11] I.C. Dikaros, E.J. Sapountzakis, Generalized warping analysis of composite beams of an arbitrary cross-section by BEM. II: Numerical applications. *Engineering Mechanics* 2014; DOI: 10.1061/(ASCE)EM.1943-7889.0000776.

[12] E.J. Sapountzakis, I.C. Dikaros, Advanced 3D beam element of arbitrary composite cross-section including generalized warping effect. *Int. J. for Numerical Methods in Engineering*, 2015, DOI: 10.1002/nme.4849.

[13] G. Giunta, S. Belourttar, A.J.M. Ferreira, A static analysis of three-dimensional functionally graded beams by herarchical modelling and collocation meshless solution method. *ActaMechanica*, 2015; DOI 10.1007/s00707-1503-3.

[14] J. Murin, M. Aminbaghai, V. Kutis, Exact solution of the bending vibration problem of the FGM beam with variation of material properties. *Engineering Structures*, **32**: 1631 – 1640, 2010.

[15] M. Aminbaghai, J, Murin, V. Kutis, Modal analysis of the FGM-beams with continuous transversal symmetric and longitudinal variation of material properties with effect of large axial force. *Engineering Structures*, **34**: 314 – 329, 2012.

[16] J. Murin, M. Aminbaghai, V. Kutis, J. Hrabovsky, Modal analysis of the FGM beams with effect of axial force under longitudinal variable elastic Winkler foundation. *Engineering Structures*, **49**: 234 – 247, 2013.

[17] J. Murin, M. Aminbaghai, J. Hrabovsky, V. Kutis, S. Kugler, Modal analysis of the FGM beams with effect of the shear correction function. *Composites: Part B*, **45**:1575–1582, 2013.

[18] V. Kutis, J. Murin, R. Belak, J. Paulech,Beam element with spatial variation of material properties for multiphysics analysis of functionally graded materials. *Computers and Structures*, **89**: 1192 – 1205, 2011.

[19] H. Rubin, Analytische Berechnung von Stäben und Stabwerken mit stetiger Veränderlichkeit von Querschnitt, elastischer Bettung und Massenbelegung nach

Theorie erster und zweiter Ordnung, *Baustatik - Baupraxis 7. Berichte der 7. Fachtagung "Baustatik - Baupraxis"* Aachen/Deutschland 18.-19. März 1999. Balkema 1999, Abb., Tab.S.135-145, in German.

[20] H. Rubin, Solution of differential equations of arbitrary order with polynomial coefficients and application to a statics problem. *ZAMM* **76**, 105 – 117, 1996.

[21] Wolfram S. MATHEMATICA 5, Wolfram research, Inc., 2003.

[22] H. Altenbach, J. Altenbach, W. Kissing,*Mechanics of composite structural elements*. Springer Verlag, 2003.

[23] J.C. Halpin, J.L. Kardos, The Halpin-Tsai equations. A review, *Polymer Engineering and Science*, **16**(5): 344 – 352, 1976.

[24] T. Reuter, G.J. Dvorak, Micromechanical models for graded composite materials: Ii. Thermomechanical loading, *Mechanics and Physics of Solids*, **46**: 1655 – 1673, 1998.

[25] J. Murin, V. Kutis, Improved mixture rules for composite (FGMs) sandwich beam finite element. *In Computational Plasticity IX. Fundamentals and Applications*. Barcelona, Spain 2007: 647 – 650.

[26] A.E. Alshorbagy, M.A. Eltaher, F.F. Mahmoud, Free vibration of a functionally graded beam by finite element method. *Applied Mathematical Modelling*, **35**: 412 – 425, 2010.

[27] M. Simsek, Vibration analysis of a functionally graded beam under a moving mass by using different beam theories, *Composite Structures*, **92**: 904 – 917, 2010.

[28] T. Rout, On the dynamic stability of functionally graded material under parametric excitation. PhD thesis. National Institute of Technology Rourkela, India. 2012.

[29] V. Kutis, J. Murin, R. Belak, J. Paulech, Beam element with spatial variation of material properties for multiphysics analysis of functionally graded materials. *Computers and Structures*, **89**: 1192 – 1205, 2010.

[30] J. Murin, S. Kugler, M. Aminbaghai, J. Hrabovsky, V. Kutis, J. Paulech, Homogenization of material properties of the FGM beam and shells finite elements. In.: *11th World Congress on Computational mechanics (WCCM XI)*, Barcelona, 20-25 July, 2014.

[31] J. Murin, M. Aminbaghai, J. Hrabovsky, V. Kutis, J. Paulech, S. Kugler, A new FGM beam finite element for modal analysis. In.: *11th World Congress on Computational mechanics (WCCM XI)*, Barcelona, 20-25 July, 2014.

[32] J. Murín, J. Hrabovský, V. Kutiš, J. Paulech, Shear correction function derivation for the FGM beams. In: *2nd International Conference on Multi-scale Computational Methods for solid and Fluids*, Sarajevo, Bosnia and Hercegovina, 10–12 June, 2015.

[33] J. Murin, M. Aminbaghai, J. Hrabovsky, V. Kutis,S. Kugler, Effect of the Shear Correction Function in the FGM Beams Modal Analysis. *In Proceedings of the 15th European Conference on Composite Materials*, Venice, Italy, 24-28 June, 2012, ISBN 978-88-88785-33-2.

[34] ANSYS Swanson Analysis System, Inc., 201 Johnson Road, Houston, PA 15342/1300, USA.

[35] H. Mang, G. Hoffstetter,*Festigkeitslehre*. Springer Verlag; 2000.